Applied Energy 254 (2019) 113690

Contents lists available at ScienceDirect

Applied Energy

journal homepage: www.elsevier.com/locate/apenergy

Perovskite thermochromic smart window: Advanced optical properties and low transition temperature

Y. Zhang[a], C.Y. Tso[b], J.S. Iñigo[c], S. Liu[b], H. Miyazaki[a], Christopher Y.H. Chao[d,*], K.M. Yu[e]

[a] Department of Mechanical and Aerospace Engineering, The Hong Kong University of Science and Technology (HKUST), Clear Water Bay, Kowloon, Hong Kong, China
[b] School of Energy and Environment, City University of Hong Kong, Tat Chee Avenue, Kowloon, Hong Kong, China
[c] TECNUN, University of Navarra, Paseo Manuel Lardizabal 13, Donostia-San Sebastian, Spain
[d] Department of Mechanical Engineering, The University of Hong Kong, Hong Kong, China
[e] Department of Physics, City University of Hong Kong, Tat Chee Avenue, Kowloon, Hong Kong, China

HIGHLIGHTS

- A perovskite smart window is designed, fabricated and investigated experimentally.
- High solar modulation ability and high luminous transmittance were achieved.
- Transition temperature is decreased with the decrease of relative humidity.
- Color versatility of perovskite smart window was discovered.
- A temperature reduction of 2.5 °C was achieved in a field test.

GRAPHICAL ABSTRACT

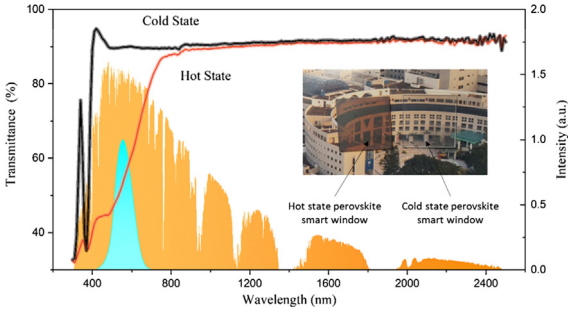

ARTICLE INFO

Keywords:
Energy efficient glazing
Perovskite
Smart window
Thermochromism
Thin film

ABSTRACT

Windows are one of the most inefficient components in buildings. Common thermochromic smart windows using VO_2 can mitigate such energy loss. However, they suffer from several problems, namely, low solar modulation ability, high transition temperature (i.e. 68 °C) and low luminous transmittance. In this study, we propose a perovskite thermochromic smart window towards achieving high solar modulation ability whilst maintaining a high luminous transmittance and a low transition temperature. Perovskite material shows a significant thermochromism in the visible and ultraviolet region. Since half of the photons lie in this spectral region, a high solar modulation can be achieved by perovskites. The material was optimized by varying the spin speed in the fabrication process as well as the mixing ratio between precursors. The optimized sample exhibits a solar modulation ability of 25.5% with luminous transmittance of 34.3% and higher than 85% in the hot (80 °C) and cold (25 °C) states, respectively, making this material suitable for practical device applications. The hysteresis loop, the transition temperature as well as transition time in relation to the relative humidity of a perovskite smart window during the heating and cooling process are investigated in this study. From field tests results, the perovskite smart window can help reduce the indoor air temperature by about 2.5 °C compared to a normal window. Overall, based on the results obtained in this study, the perovskite thermochromic smart window has potential to achieve excellent thermochromic properties, providing an alternative to alleviate the high energy consumed in buildings.

* Corresponding author at: Department of Mechanical Engineering, The University of Hong Kong, Pokfulam Road, Hong Kong, China.
E-mail address: cyhchao@hku.hk (C.Y.H. Chao).

https://doi.org/10.1016/j.apenergy.2019.113690
Received 31 January 2019; Received in revised form 12 July 2019; Accepted 2 August 2019
Available online 13 August 2019

Nomenclature

SHGC	solar heat gain coefficient [–]
FDTD	finite difference time domain [–]
LCST	lower critical solution temperature [°C]
MIT	metal-insulator transition [–]
NIR	near infrared [–]
TC	thermochromic [–]
PMMA	poly(methyl methacrylate) [–]
T_{lum}	luminous transmittance [%]
ΔT_{sol}	solar modulation ability [%]
$T_{lum,cold}$	luminous transmittance in cold state [%]
$T_{lum,hot}$	luminous transmittance in hot state [%]
T_c	transition temperature [°C]
ΔT_c	hysteresis width [°C]
$T_{c,h}$	transition temperature in heating process [°C]
$T_{c,c}$	transition temperature in cooling process [°C]
UV	ultraviolet [–]
λ	wavelength [nm]

1. Introduction

A better trade-off technique should be implemented to maintain thermal comfort levels for residents in buildings but with reduced energy usage by preventing unnecessary loss. Windows are widely recognized as one of the most inefficient elements. Not only is heat lost (or gained) through windows by thermal transmission, but incident solar radiation also has a detrimental effect by heating the room in summer. Grynning et al. [1] found that the heat loss related to windows accounted for 45% of the total heat loss through the building envelope for a typical Norwegian office building.

So, regulating the heat through the window becomes an important consideration in building design. Smart windows are advanced technologies that can modulate the solar short-wavelength radiation and therefore can be used to mitigate such energy loss. Smart windows are coated with materials which are able to tune the light transmittance in a certain range of solar radiation such as ultraviolet (UV), visible, and near-infrared (NIR), dynamically and reversibly in a "smart way". There is another term called adaptive facades which are building envelopes that are able to adapt mechanically or chemically to external climate conditions on a daily, seasonal or yearly basis to meet internal loads and occupant needs [2]. The smart window is one category of adaptive facade that uses its coating's chemical or physical properties to achieve the reversible adaptation to the external environment. For smart windows, light transmission properties can be controlled by the application of a voltage (electrochromism) [3], light (photochromism) [4], or heat (thermochromism). Among them, thermochromic smart windows are highly competitive due to their unique characteristics: low cost, passivity and rational stimulus response [5]. This paper focuses on thermochromic smart windows using a thermochromic perovskite material which is highly transparent in the cold state and shows large solar modulation ability and low transition temperature. This paper aims to answer the questions; Are there advantages these windows can provide for the residents in building? What disadvantages need to be further improved to make perovskite thermochromic smart windows better for practical application? Also, the most important question: Can these windows indeed save energy in the field test?

Vanadium dioxide (VO_2) is the most widely studied material for smart windows [6] because of its thermochromic behavior coming from the Metal-Insulator Transition (MIT) of the material at a tunable transition temperature. The reversible phase transition of VO_2 involves an abrupt change in near-infrared transmittance, which makes VO_2 an attractive candidate for smart window applications. However, several drawbacks of VO_2 for smart windows are hindering further development. Due to absorption in the visible range in both the semiconducting and the metallic states, VO_2 has a low luminous transmittance (T_{lum}) of ~50%. Energy saving using VO_2 thermochromic windows is not efficient because its thermochromic effect is only in the near infrared region ($\lambda > 900$ nm) giving rise to a low solar modulation ability (ΔT_{sol}). Moreover, VO_2 has a high transition temperature of ~68 °C. Other challenges include the intrinsic yellow-brown color of the material, its low resistance to oxidization and laborious control of the fabrication process.

To address the deficiencies of VO_2 as an efficient thermochromic window material, some novel temperature-response materials with desirable thermochromic properties needed to be urgently explored. Recently, thermochromic hydrogel and ionogel have attracted considerable attention as candidates for thermochromic smart window applications. For hydrogel, a drastic transmittance change takes place in the 250 to 1800 nm-range, induced by a hydrophilic to hydrophobic transition. The extensively studied thermochromic hydrogels include polyampholyte hydrogel (PAH) [7], poly(N-isopropylacrylamide) (PNIPAm) [8], and hydroxypropyl cellulose (HPC) [9]. The thermochromic property of ionogel is based on an octahedral (low temperatures)-tetrahedral (high temperatures) configuration change of transition metal complexes assisted by interaction with donor solvent molecules, resulting in a strong absorption at higher temperature and a favorable thermochromic response [10,11]. However, some challenges are faced with hydrogel and ionogel thermochromic materials. A rigorous encapsulation is required because of the liquid phase nature. During their utilization, leaks of thermoresponse material could appear followed by a dramatic decrease in performance [5].

Consequently, to reach a smart window suitable for practical applications, several points should be considered: firstly, the "ideal" smart window must remain in the solid state with suitable T_{lum}, high ΔT_{sol} with a low transition temperature near room temperature. There are no regulations for architectural windows in terms of T_{lum}. High T_{lum} windows can give residents both positive and negative experiences [12]. On the one hand, the primary role of a window is to provide a visual portal for residents to external environments, and high transmittance is needed to save energy for lighting in the day time. On the other hand, more daylight through high T_{lum} windows is accompanied by increased solar gains (thermal discomfort) and glare. Glare is a source of visual discomfort and can be defined as the contrast lowering effect within a visual field due to the presence of bright light sources [13]. The glare can be an impediment to vision and even a direct hazard as it can cause serious or mild discomfort. Even minor effects may accumulate, as with a low but incessant noise, to lead to fatigue during the working day [14]. Therefore, excessive glare should be reduced so as not to disturb residents. For automobile wind shields, the legal guidelines indicate the minimum T_{lum} must be greater than 70% in parts of United States, Europe and Russia [15]. The ΔT_{sol} has a strong relationship with the energy saving potential of a thermochromic smart window and the larger solar modulation is especially helpful in warmer climates. There is no systematic study of a visible solar spectrum regulating window, but the optimum transition temperature of a NIR solar spectrum regulating window should be around 21 °C [16]. Transition time should also be considerably fast (within several minutes [5]) to achieve instant response.

Thermochromic properties of perovskite materials have recently been reported. Halder [17] explored the thermochromic behavior of hydrated lead halide hybrid perovskites $CH_3NH_3PbI_3$ and attributed the thermochromism of perovskite to the reversible hydration/dehydration process of $CH_3NH_3PbI_3$ when it encounters moisture.

$$CH_3NH_3PbI_3 + 3CH_3NH_3I \overset{H_2O}{\leftrightarrow} (CH_3NH_3)_4PbI_6{\cdot}2H_2O, \text{ [17]} \quad (1)$$

A chemical equation (Eq. (1)) has been derived based on XRD results of thin film materials before and after the hydration/dehydration process. As illustrated in Fig. 1, at the cold state the dehydrated perovskite $(CH_3NH_3)_4PbI_6{\cdot}2H_2O$ is in a non-perovskite phase. On the other hand, at the hot state it becomes a normal organic-inorganic lead halide perovskite $CH_3NH_3PbI_3$, Following this pioneer work, Lin et al. [18] developed a smart photovoltaic window using the $CsPbI_{3-x}Br_x$ perovskite material. The photovoltaic window can change from a transparent cold state with 81.7% visible transparency to a colored hot state with 35.4% visible transparency. A device efficiency above 7% has been achieved in these thermochromic photovoltaic windows in the hot state. Combining two state-of-the-art technologies, smart window technology and solar cell technology, into one window will achieve the two targets of energy saving and energy generation in the same device, which is a very interesting and important topic that needs to be explored. However, their thermochromic solar cells showed a high transition temperature (100–350 °C) and a long transition time (up to 25 h).

According to Table 1, compared to VO_2 thermochromic smart windows, perovskite thermochromic smart windows are highly transparent in the cold state and the thermochromism takes place in the visible region where half of the phonons lie. These properties imply a high luminance transmittance and ΔT_{sol} for perovskite thermochromic smart windows. As for hydrogel and ionogel thermochromic smart windows, thermochromic perovskite is solid phase and does not need rigid encapsulation. Based on these reasons, a perovskite thermochromic smart window is thought to have some superior properties over VO_2, hydrogel and ionogel.

In order to further explore these smart thermochromic perovskite windows, a general understanding of the thermochromism of perovskite is needed. Previous studies only reported the thermochromic ability of $CH_3NH_3PbI_3$ perovskite material, leaving the quantification of the major parameters of thermochromism (optical properties and transition process properties) unstudied. These parameters are essential to determine whether perovskite thermochromic windows can save energy and how much energy can be saved. The transition temperature and transition time of $CsPbI_{3-x}Br_x$ thermochromic perovskite windows is too high and too long respectively and the transition properties of thermochromic $CH_3NH_3PbI_3$ perovskite are unknown. How to control the transition temperature and transition time in a reasonable range for real application needs to be solved. The fabrication process also needs to be explored. In addition, if these windows have good thermochromism performance, it remains unclear whether the environment will influence the windows.

In this study, we aim to give a full picture of $CH_3NH_3PbI_3$ as a material for thermochromic smart windows in order to assess real field application. The major parameters related to the thermochromic effect such as T_{lum} and ΔT_{sol} are first quantified. The influence of the mixing ratio of two ingredients along with the spin speed during fabrication are investigated and reported in Section 3.1. A transmittance spectrum of the perovskite smart window is discussed in Section 3.2. The results of hysteresis properties as well as transition temperature are presented in Section 3.3, meanwhile the relationship between relative humidity and transition time of the perovskite smart window are shown in Section 3.4 Finally, the color versatility of the perovskite smart window is discussed (Section 3.5) and the energy saving property of the perovskite smart window in a practical application is examined through an experiment with a model house under real environmental conditions (Section 3.6). A comparison with other thermochromic smart windows is addressed at the last section. Overall, this study will help to characterize some optical properties of the perovskite material, understand the principle of perovskite thermochromism and discuss the possibility of a novel perovskite material for thermochromic smart windows to solve the high energy consumption issue in buildings.

2. Materials and methods

2.1. Smart window fabrication

Perovskite can only be deposited on a substrate that has good wettability with the solvent (N, N-Dimethylformamide, namely, DMF) of the perovskite precursor [30]. Hence, perovskite cannot be deposited on quartz directly because of the high contact angles of DMF on bare quartz. A SiO_2 thin film was first deposited on quartz substrates as a buffer layer for its environmentally friendly property (easily fabricated without high temperature to process). The SiO_2 thin film was fabricated through a facile sol-gel method. The SiO_2 sol was prepared by the hydrolysis of tetraethyl orthosilicate ($Si[C_2H_5O_4]$, abbreviated as TEOS, ≥ 99.0%, Sigma-Aldrich) in ethanol in the presence of ammonia as a catalyst. This is commonly known as the modified Stöber growth method, introduced in 1968 by Werner Stöber, for preparing

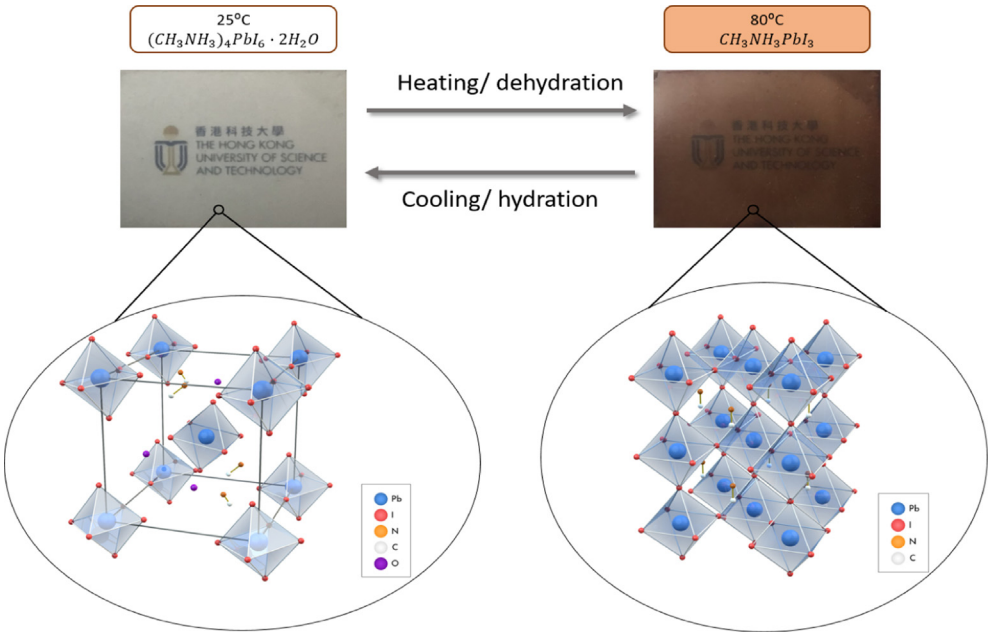

Fig. 1. Schematics of the cold to hot state transition by heating (dehydration) and the hot to cold state by cooling (hydration).

Table 1
Summary of the existing thermochromic materials.

Thermochromic materials	Enhanced strategies/Different materials	Thermochromic properties	Challenges	Refs.
Vanadium dioxide	Chemical doping	Mg: T_{lum} = 47.5%, ΔT_{sol} = 12.8% Sr: T_{lum} = 64.2%, ΔT_{sol} = 6.7%	Low T_{lum}, low ΔT_{sol} and high intrinsic transition temperature	[19,20]
	Porosity	T_{lum} = 41.6%, ΔT_{sol} = 14.1%		[21]
	Antireflection layer	ZrO_2: T_{lum} = 50.5% TiO_2: T_{lum} = 44.0% Index-tunable: T_{lum} = 44.0% ΔT_{sol} = 18.9%		[22–24]
	Composite	T_{lum} = 53.0%, ΔT_{sol} = 11.7%		[25]
	Nanogrid	FDTD simulations: T_{lum} = 76.5%, ΔT_{sol} = 14.0% Experiments: T_{lum} = 67.0%, ΔT_{sol} = 8.8%		[26,27]
	Bioinspired Moth Eye	FDTD simulations: T_{lum} = 70.3%, ΔT_{sol} = 23.1% Experiments: T_{lum} = 44.5%, ΔT_{sol} = 7.1%		[15,28]
Hydrogels	PNIPAm	$T_{lum,hot}$ = 59.9%, $T_{lum,cold}$ = 87.9%, ΔT_{sol} = 20.4%	Liquid phase requires rigorous encapsulation	[8]
	VO_2/PNIPAm	$T_{lum,hot}$ = 43.2%, $T_{lum,cold}$ = 82.1%, ΔT_{sol} = 34.7%		[29]
Ionogel	IL-Ni-Cl	$T_{lum,hot}$ = 15%, $T_{lum,cold}$ = 87.0%, ΔT_{sol} = 50%	Liquid phase requires rigorous encapsulation	[11]

monodispersed spherical silica [31,32]. In this procedure, 5 mL ammonia $NH_3{\cdot}H_2O$ and 100 mL ethanol were mixed with 3 mL TEOS under constant stirring at 60 °C for 12 h [33]. The obtained colloidal solution was the SiO_2 sol. A one-step method was used to fabricate the perovskite precursor. A certain amount of PbI_2 (99%, Sigma-Aldrich), CH_3NH_3I (DYESOL), and CH_3NH_3Br (DYESOL) were dissolved in DMF solvent (≥99%, Sigma-Aldrich) under vigorous stirring in a water bath at 50 °C for 48 h. [17]. The exact amount of chemicals for the perovskite precursor with different mole ratio ingredients can be found in Table 2.

Fused quartz and glass slide substrates with the dimension of 3 cm × 3 cm × 1 mm (the fabrication method of SiO_2 thin film and perovskite thin film is spin-coating. The minimum substrate size for the spin coater is 3 cm × 3 cm and the thickness of the commonly used fused quartz and glass slide is 1 mm) were cleaned consecutively with deionized (DI) water, ethanol, and acetone in an ultrasonic bath. The perovskite precursor was spin-coated on the substrate with a low rate of 400 rpm for 6 s and a high rate of 2000 to 5000 rpm for 30 s. Then, the sample was dried on a hot plate at 90 °C for 15 min to remove the excess solvent. The fabrication process is illustrated in Fig. 2. A schematic diagram of a perovskite thermochromic smart window and a photograph of perovskite smart windows in the "hot" (right) and "cold" (left) states is shown in Fig. 3.

2.2. Characterization

The transmission measurements were conducted at a spectral range of 300 to 2500 nm using a UV–vis-NIR spectrophotometer (Lambda 950, Perkin Elmer, USA). This spectrophotometer is equipped with an integrating sphere accessory. The sample was placed in front of the sphere entrance port through which the light beam enters the sphere, collecting all the light passing through the sample. The transmittance measured by this method refers to the total transmittance, implying that it includes both the specular transmittance and the diffuse transmittance. A home-built temperature controller was used to manipulate the sample temperature for a transmission measurement at different temperatures (25 °C and 80 °C for cold state and hot state). The unit consists of a kapton resistive heater, a Diqi-Sence PID temperature controller and a T-type thermocouple, which form a closed loop to control the temperature of the smart windows. The sample temperature was measured using a T-type thermocouple taped directly by aluminum tape onto the film surface. The transmittance curve of a quartz slide was calibrated as the baseline using software (UV WinLab^{TM}). To quantify the amount of visible light transmitted by the windows is useful for human vision under normal conditions, the luminous transmittance T_{lum} is defined in Eq. (2). Similarly, to quantify the amount of solar thermal energy entering a building via solar transmittance, solar transmittance T_{sol} is defined in Eq. (3). The solar modulation ability ΔT_{sol} is then defined in Eq. (4) as ΔT_{sol}.

$$T_{lum} = \frac{\int_{\lambda=380nm}^{780nm} \bar{y}(\lambda)T(\lambda)d\lambda}{\int_{\lambda=380nm}^{780nm} \bar{y}(\lambda)d\lambda} \tag{2}$$

$$T_{sol} = \frac{\int_{\lambda=300nm}^{2500nm} AM_{1.5}(\lambda)T(\lambda)d\lambda}{\int_{\lambda=300nm}^{2500nm} AM_{1.5}(\lambda)d\lambda}, \tag{3}$$

$$\Delta T_{sol} = T_{sol}^{cold} - T_{sol}^{hot} \tag{4}$$

where $T(\lambda)$ is the transmittance of the smart windows at wavelength λ. The CIE (International Commission on Illumination) standards for photopic luminous efficiency of the human eye ($\bar{y}(\lambda)$), and the solar irradiance spectrum for an air mass of 1.5 ($AM_{1.5}(\lambda)$) were used as weighting functions for the wavelength dependent transmittance. The

Table 2
Exact amount of chemicals used in experiments.

Precursors	PbI_2(g)	CH_3NH_3I(g)	CH_3NH_3Br(g)	DMF (mL)
PbI_2: CH_3NH_3I=1:4	0.807	1.1128	0	2.5
PbI_2: CH_3NH_3I=1:6	0.807	1.6692	0	2.5
PbI_2: CH_3NH_3I=1:8	0.807	2.2256	0	2.5
PbI_2: CH_3NH_3I=1:10	0.807	2.7820	0	2.5
PbI_2: CH_3NH_3I: CH_3NH_3Br = 1:3:1	0.807	0.8348	0.196	2.5
PbI_2: CH_3NH_3I: CH_3NH_3Br = 1: 2: 2	0.807	0.5565	0.392	2.5
PbI_2: CH_3NH_3I: CH_3NH_3Br = 1: 1: 3	0.807	0.2783	0.588	2.5
PbI_2: CH_3NH_3Br = 1: 4	0.807	0	0.784	2.5

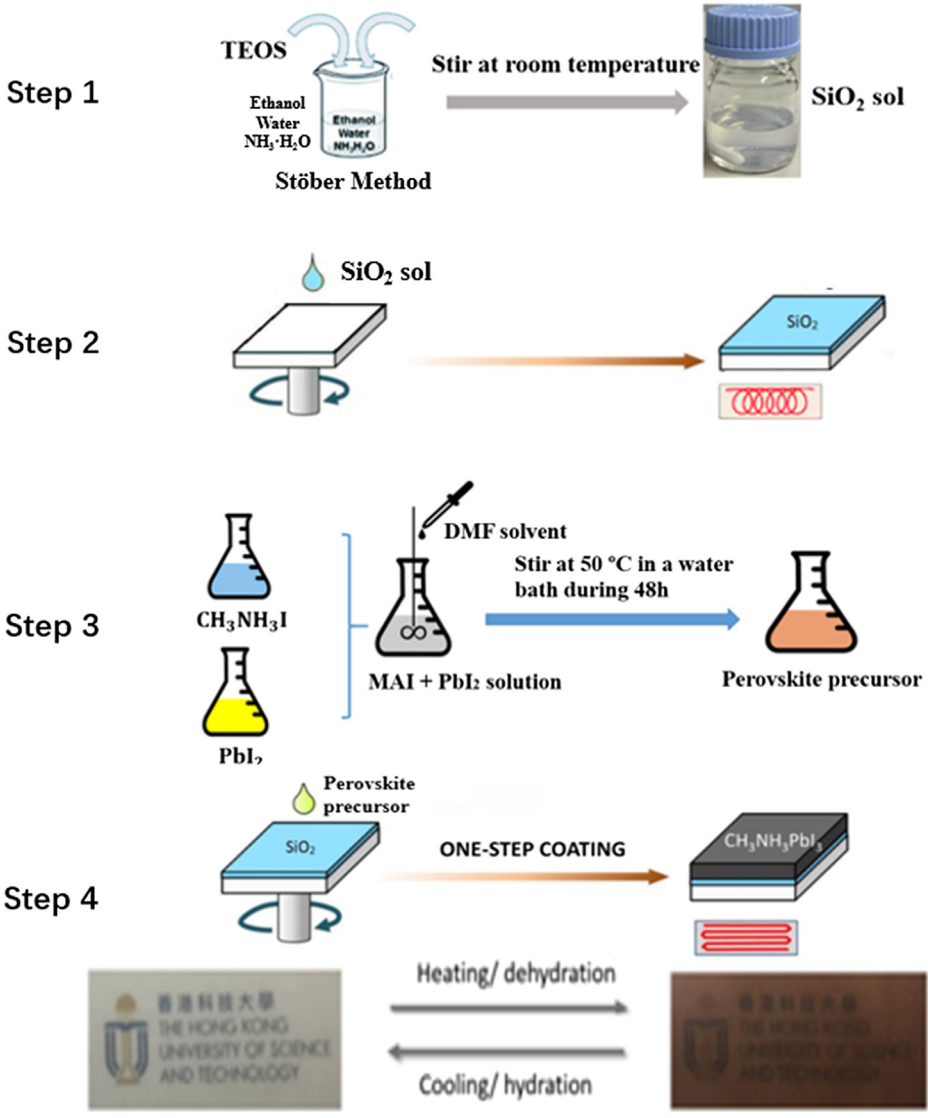

Fig. 2. A schematic of the fabrication process of a perovskite thermochromic smart window. There are four steps to fabricate a perovskite thermochromic smart window. Step 1 is to prepare the SiO_2 precursor using the Stöber method, followed by step 2 to fabricate SiO_2 thin film. Step 3 is to prepare the thermochromic perovskite precursor (the mixing ratio of PbI_2 and CH_3NH_3I is 1:4). Step 4 is to use the one-step method to deposit thermochromic perovskite on SiO_2 buffer layer.

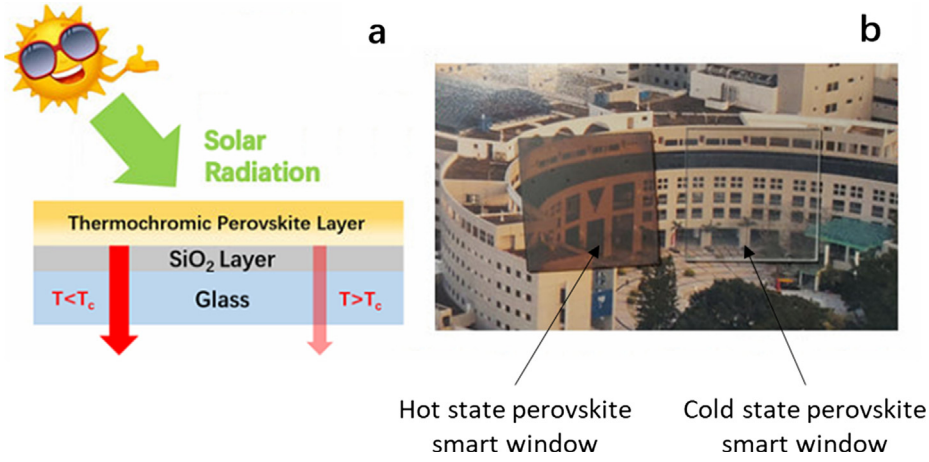

Fig. 3. (a) A schematic diagram showing a perovskite thermochromic smart window; (b) Photograph of the cold state (non-coloured) and hot state (brown coloured) perovskite smart windows. The windows in cold state are highly transparent and the windows in hot state are brown, however, objects can still be seen clearly through the windows.

wavelength range used for T_{lum} is 380 nm ≤ λ ≤ 780 nm corresponding to the limits of human vision. The $AM_{1.5}$ was chosen for solar averaged transmittance calculations as it represents an overall yearly average for mid-latitudes including diffuse light from the ground and sky on a south facing surface tilted 37° from horizontal. The wavelength range used for these calculations is 300 nm ≤ λ ≤ 2500 nm which accounts for 99.2% of terrestrial solar energy. It should be noted that the transmission spectra results presented in this study are averaged values of at least three repeated experiments, and the error bars represent standard deviations of the collected data.

3. Results and discussion

3.1. Tunable luminous transmittance in hot state and solar modulation ability by different mixing ratio and spin speed during fabrication

The thermochromic behavior of $CH_3NH_3PbI_3$ perovskite is apparent when the relative molar concentration of CH_3NH_3I is higher than PbI_2. Furthermore, when the precursor solution consists of 1:4 M concentrations of PbI_2 to methylammonium iodide (CH_3NH_3I), the coating can be turned completely transparent in a cold state [17]. The thermochromism of perovskite is caused by the unequal ratio of the two ingredients. Consequently, the behavior when the mixing ratio further increases needs to be explored. The results in Fig. 4 show all the mixing ratios. The $T_{lum,cold}$ does not change significantly and all maintain a high value (~90%) (i.e. the spin speed is 2000 rpm for all the different mixing ratio experiments). To account for the diffuse transmittance of the samples, an integrating sphere was used to measure the hemispherical transmittance. It is for this reason that the perovskite smart windows appear slightly opaque to the human eye, despite an inherently high transmittance. The thermochromic property still exists with the increase of the mixing ratio of CH_3NH_3I to PbI_2; hence, the $T_{lum,hot}$ and solar modulation can be precisely controlled by changing the mixing ratio. The $T_{lum,hot}$ increases while the ΔT_{sol} decreases with the mixing ratio. Through adjustment of the mixing ratio of CH_3NH_3I and PbI_2, the highest $T_{lum,hot}$ of 59.4% with ΔT_{sol} of 12.7% is achieved, while the highest ΔT_{sol} can reach 25.5% withT_{lum} = 34.3% in the hot state.

Fig. 5 shows XRD patterns of perovskite samples with different precursor ratios. The prominent diffraction peak at $2\theta = 11.39^{\circ}$ in all the samples and is consistent with the characteristic peak from dihydrated perovskite [34], implying that a dominant fraction material in the cold state is in the dihydrated perovskite phase. The presence of PbI_2 has been known to be associated with perovskite degradation. However, from XRD results, no detectable PbI_2 in the cold state is present. This is consistent with our observation that the hydration-dehydration process in these samples is totally reversible. In all the different mixing ratios, there is no peak corresponding to diffractions from the $CH_3NH_3PbI_3$ perovskite phase, suggesting that the transition of hydration-dehydration is complete and no residual $CH_3NH_3PbI_3$ phase is present in the cold state. It is worth noting that all the samples show only diffraction from hydrated perovskite and the CH_3NH_3I. With increasing CH_3NH_3I in the precursor, more CH_3NH_3I phase is present in the sample as is evident from the strong CH_3NH_3I diffraction peaks. Hence, the mixing ratio of 1:4 of PbI_2 and CH_3NH_3I is chosen for further experiment.

According to Beer-Lambert's law, the thickness of a coating has a strong effect on the transmittance. So, the optical properties of perovskite can be modified due to the thickness of the perovskite coating by changing the spin speed of the spin coater from 2000 rpm to 5000 rpm in the fabrication process. Fig. 6 shows the trend of $T_{lum,hot}$ and ΔT_{sol} according to the spin speed. The $T_{lum,hot}$ increases and the ΔT_{sol} decreases as the spin speed increases, corresponding to a reduction in the film thickness. Once the spin speed achieves values near 5000 rpm, the $T_{lum,hot}$ reaches 53.2% although the ΔT_{sol} ability drops to 14.5%. Samples with the highest ΔT_{sol}, which correspond with a spin speed of 2000 rpm, are chosen for further investigation later in this work since higher ΔT_{sol} leads to higher energy savings, which is the purpose of a thermochromic smart window. Similarly, for all the spin speeds studied, the $T_{lum,cold}$ does not change significantly and all maintain a high value (~90%).

3.2. Transmittance spectrum of perovskite smart window

Fig. 7 shows the transmittance spectra of the perovskite smart window in the cold (25 °C) and hot states (80 °C) at ambient relative humidity (around 60%). The main difference in the transmittance occurs in the visible (380–780 nm) and ultraviolet regions (300–380 nm), with a small contribution from the near infrared region. The UV and visible light account for about 57% of the solar energy in the solar spectrum (yellow filled spectrum in Fig. 7). This indeed is the reason that the ΔT_{sol} of the perovskite smart window can be as large as 20–30%. Due to the region in which thermochromism takes place, the ΔT_{sol} highly depends on the $T_{lum,hot}$. That means, if the ΔT_{sol} increases, the $T_{lum,hot}$ decreases. However, for the perovskite smart window, the results show a potential trade-off between the T_{lum} and ΔT_{sol}, which other types of smart windows cannot achieve. In this study, perovskite smart windows can be optimized to achieve $T_{lum,hot}$ = 36.0%, $T_{lum,cold}$ = 89.1% and ΔT_{sol} = 25.4%. These performance figures are very promising when compared to all the other smart windows.

3.3. Hysteresis properties and transition temperature of a perovskite smart window

A hysteresis loop of transmittance-temperature exists in the heating/cooling cycles of a perovskite smart window. Studying the hysteresis loop is essential to explain the transition process of the perovskite material. The transition hysteresis of a thermochromic material is always considered to have a detrimental effect on the performance. Because the hysteresis loop exists, the real transition temperature will deviate from the average temperature. The transmittance and hysteresis loops of perovskite coatings (at 550 nm wavelength) have been collected under variable temperatures at intervals of 2 °C and are shown in Fig. 8. This phenomenon can be attributed to the energy barrier being different between the heating and cooling process (dehydration and hydration process). Transmittance at the wavelength of 550 nm was chosen to monitor the thermochromic effect since the biggest difference in the transmittance of perovskite is observed at 550 nm (Fig. 7), and at the same time, 550 nm also corresponds to the peak in CIE photopic luminous efficiency of the human eye. From the transmittance-

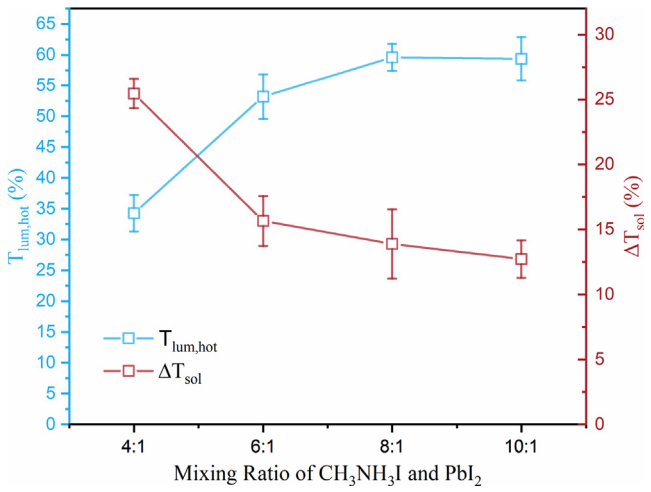

Fig. 4. $T_{lum,hot}$ and ΔT_{sol} as a function of different precursor ratios. The highest $T_{lum,hot}$ is 59.4% with ΔT_{sol} of 12.7%, while the highest ΔT_{sol} can reach 25.5% with $T_{lum,hot}$ of 34.3%.

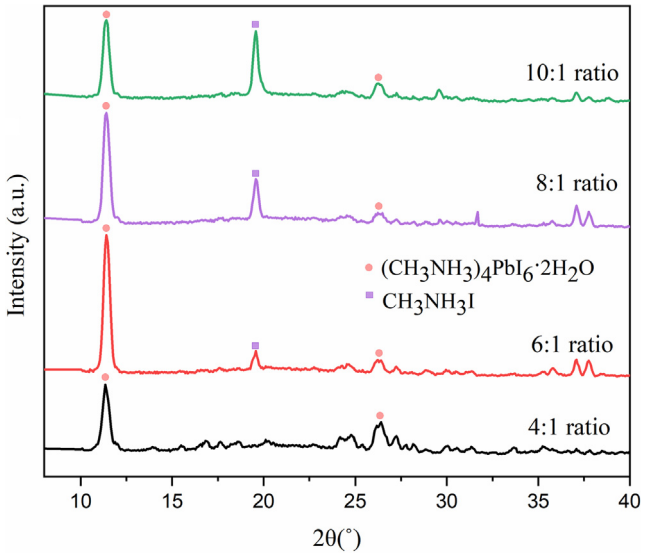

Fig. 5. XRD results of different ratio perovskite smart windows. In all the different mixing ratios, there is no peak corresponding to diffractions from the $CH_3NH_3PbI_3$ perovskite phase, suggesting that the transition of hydration-dehydration is complete.

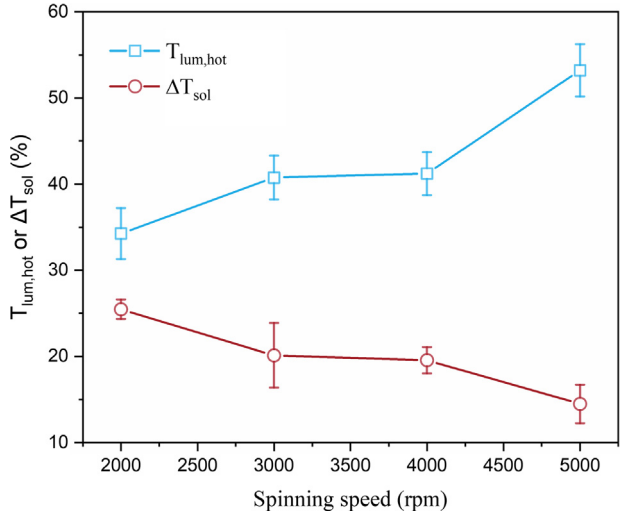

Fig. 6. Trend of $T_{lum,hot}$ and ΔT_{sol} at 80 °C for different spin speeds during fabrication process. Increasing the spin speed will increase the luminance transmittance while decreasing the ΔT_{sol}.

temperature data, the transition temperature of the heating and cooling cycles ($T_{c,h}$, $T_{c,c}$respectively), the average transition temperature ($T_c = \frac{T_{c,h} + T_{c,c}}{2}$) and the width of the hysteresis loop, $\Delta T_c = T_{c,h} - T_{c,c}$ can be calculated. As the hysteresis loop is unfavorable for a thermochromic material for smart window applications, a small ΔT_c is desirable. Simulation studies suggest that reducing the width of the hysteresis loop can improve the energy savings to some degree [35].

The transition parameters for these coatings are summarized in Table 3, where it can be seen that the transition temperature of the perovskite smart window is lower than that of the traditional VO_2 smart window (~68 °C). Since the thermochromic effect comes from the hydration and dehydration process as illustrated in Eq.1, it is expected that humidity plays a crucial role in transition temperature and the hysteresis loop. We have also studied the effect of the relative humidity of the environment on the transition processes of the samples and results are shown in Fig. 9. Fig. 9(a) shows that by decreasing the relative humidity of the environment, the average transition temperature decreases from 53.7 °C to 42.5 °C. The higher transition temperature at higher ambient humidity is intuitive since water molecules in the environment can hinder the dehydration process of the hydrated perovskite, requiring a higher temperature to help the hydrated perovskite lose the water molecules. This can also be explained by the chemical equilibrium of Eq.1. During the dehydration process, the system produced water, so a high humidity condition is not favorable to the dehydration process. Therefore, a high temperature is needed for the high humidity condition to let hydrated perovskite successfully dehydrate. Therefore, humidity can also be exploited to control the transition temperature of perovskite smart windows by over 10 °C. It is also worth noting that the humidity influences the hysteresis width. From Fig. 9(b), it can be seen that the hysteresis width decreases with the increase in relative humidity.

3.4. The relationship between relative humidity and transition time of a perovskite smart window

Although the transition time of a thermochromic material has drawn much less attention than the solar modulation or the transition temperature, considering the temperature fluctuation in a day, faster switch properties are preferred. Therefore, the transition time for the thermoresponsive material is also an important factor for smart window applications. To date, there remains no consensus on the desirable switch time, but it is generally agreed that a switch time within several minutes should be acceptable for an energy-saving window [5].

Both transition times from cold to hot state ($\tau_{c\rightarrow h}$) and from hot to cold state ($\tau_{h\rightarrow c}$) were investigated with relative humidity ranging from 35 to 85%. First, the transition time from the cold state to hot state ($\tau_{c\rightarrow h}$) showed no observable dependence on relative humidity values and stayed below 60 s. On the other hand, we found that the transition time between hot to cold state $\tau_{h\rightarrow c}$ strongly depends on the relative humidity. When the relative humidity is below 45%, $\tau_{h\rightarrow c}$ is more than 30 mins since the perovskite needs more time to absorb enough water to return to the hydrated state. Fig. 10 shows the strong dependence of the transition time $\tau_{h\rightarrow c}$ on the relative humidity: for relative humidity > 45%, $\tau_{h\rightarrow c}$ decreases sharply from a few minutes to ~30 s when relative humidity is ~85%. This is in good agreement with the results reported by Lin et al. [18]. Although this result suggests that there exists a critical relative humidity between 35 and 45% where $\tau_{h\rightarrow c}$ drops drastically from > 30 min to ~5 min with increasing relative humidity, it is worth noting that the stability of the perovskite smart window degrades when the environmental relative humidity is too high.

Also, the dependence of transition temperature on humidity presented in Section 3.3 shows that, for relative humidity higher than 80%, the transition temperature will be too high for practical applications. Consequently, there is a trade-off between transition time and transition temperature. A relative humidity between 40% and 60% for our developed perovskite will result in optimum smart window performance with transition temperature below 42.5 °C and transition time of several minutes.

Based on this special transition property of perovskite, a window configuration was proposed to lower the transition temperature for practical application. The configuration is similar to the conventional double-glazing window. However, the perovskite film can be coated on the inner faces of the panels, and air or argon of a certain relative humidity can fill the gap to keep the desired transition temperature for the perovskite film. In this way, a higher degree of freedom can be achieved by residents in order to control the transition process of the smart window. In practical applications, by setting the desired humidity, the user could decide the transition temperature of the window depending of their needs. When humidity inside the gap is set as a high value, the transition temperature will be high, so the window will remain in transparent state for most of the time, allowing residents to connect with the outside world. Conversely, if the humidity of the filled

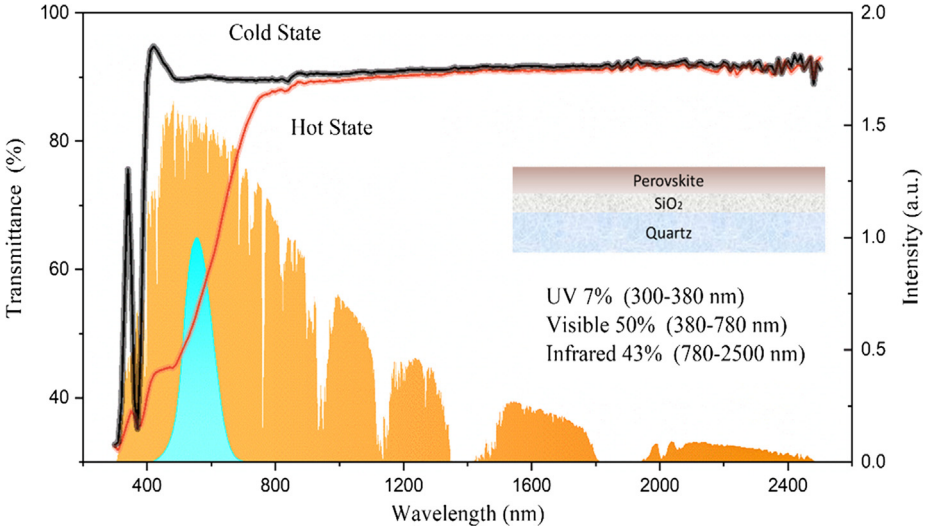

Fig. 7. The transmittance spectrum of a perovskite smart window [yellow filled spectrum is the solar intensity spectrum, while the blue filled spectrum represents the photopic luminous efficiency of the human eye].

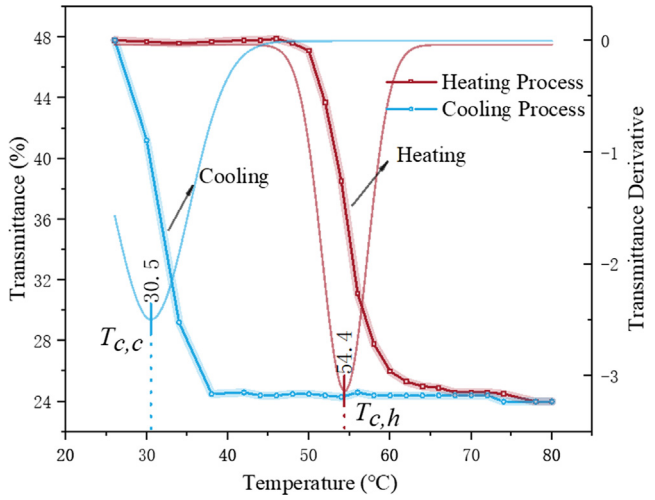

Fig. 8. The temperature-dependent thermochromic hysteresis loop (measured at 550 nm) of the perovskite smart window upon heating and cooling processes.

Table 3
Key parameters of the hysteresis loop of perovskite smart windows under different relative humidity.

Relative Humidity	Transition Temperature (°C)		Average Transition Temperature (°C)	Hysteresis Width $\Delta T_c = T_{c,h} - T_{c,c}$ (°C)
	Heating	Cooling		
35%	51.2	/	/	/
60%	54.4	30.5	42.5	23.9
71%	59.2	39.1	49.2	20.1
87%	62.5	44.8	53.7	18.5

gas is low, the transition temperature will be low; therefore, a great energy reduction will be achieved. The certain relative humidity of the filled gas can be set in the manufacturing process according to customer requirements. This kind of configuration can also protect the perovskite film from the unstable environment in the long-term operation. At the same time, the outer faces of the glazing are ready to integrate other technologies, such as self-cleaning function.

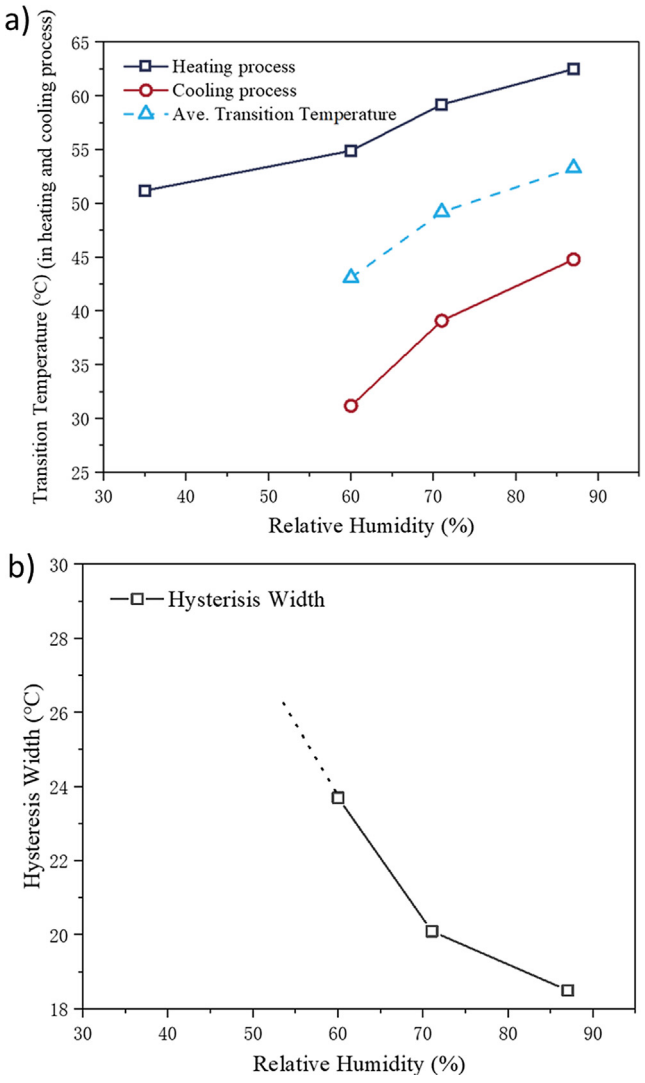

Fig. 9. (a) Effect of relative humidity on transition temperature; (b) Effect of relative humidity on hysteresis width.

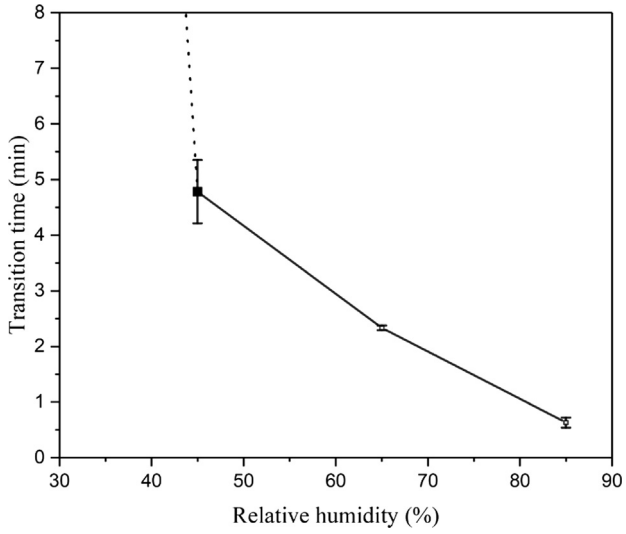

Fig. 10. Effect of relative humidity on transient time of $CH_3NH_3PbI_3$.

3.5. Versatility of perovskite smart window

In addition to the relatively low transition temperature, fast transition time and large solar modulation, perovskite smart windows also show great potential for color versatility. In VO_2 thermochromic smart windows, doping [36], photonic crystal [37] and incorporating metal nanoparticles [38] are commonly used to modify the intrinsic brown-yellowish color of VO_2 smart windows. However, changing the color of VO_2 thin film by applying various methods in the film synthesis always comes with some drawbacks, such as degradation of solar modulation performance and costly complex fabrication processes. Inspired by the continuously tunable bandgap of $CH_3NH_3PbI_{3-x}Br_x$ between 1.55 and 2.3 eV by changing the alloy composition (i.e. x = 0–3), we also change the color of the perovskite smart window by varying halide composition between iodide and bromide. This enables the color to change continuously from dark brown to bright yellow due to an increase in the bandgap of the perovskite material (shown in Fig. 11). All the perovskite material in this experiment can be written as $CH_3NH_3PbI_{3-x}Br_x$, and the results show that the higher the value x, the lighter the colour would be. Additionally, the thermochromism of perovskite smart windows still exists. In terms of the aesthetic property of windows, opinions differ: a perovskite smart window offers a chance for residents to choose the colour of their thermochromic smart window from light yellow to dark brown, which is not possible with other kinds of thermochromic smart windows.

3.6. Scale-up fabrication of perovskite smart window and model house experiments

Based on the facile fabrication routine of perovskite smart windows, it is not difficult to scale up using roll to roll tape-cast process for mass production of commercial smart windows. Researchers have tried to use various kinds of scalable solution processes to fabricate perovskite solar cells, such as roll to roll [39], inkjet printing [40] and blade coating [41]. A 90 × 90 mm smart window was fabricated for demonstration (90 × 90 mm is the largest sample size that our spin coater can process). To quantitatively evaluate the performance of a perovskite smart window for autonomous solar energy blocking in a real situation, two heat-insulated poly(methyl methacrylate) (PMMA) model houses were built and placed directly under sunlight, to mimic the real application, as shown in Fig. 12. Each model house had a volume of 12 × 12 × 9 cm^3 (i.e. 1296 cm^3) with a window of 9 × 9 cm^2 (i.e. the window to wall ratio is 56.3%, which is the number between the ratio of a glass curtain wall and a normal residential wall [42]). The smart window with perovskite layers was attached to one of the model houses, while the other model house had normal glass windows as a reference. The rooms were sealed during the testing process. The model houses were placed on the rooftop of a building in Hong Kong. Two T-type thermocouples were employed to measure the temperature inside the houses. Many studies have been conducted using similar methods to prove the energy saving of thermochromic smart windows [434445]. Actual solar radiation was used in this study to test the performance of the perovskite thermochromic smart window, evaluating the temperature reduction inside a model house in summer.

The first test results (Fig. 13.a) illustrate that after 10:00 am in fall (04/10/2018, average relative humidity: 55%), the application of the perovskite smart window caused a temperature reduction inside the house. As the sun's radiation increased, the temperature difference increased gradually and stabilized at about 11:00 am. The maximum temperature reduction during the whole day was about 2.5 °C. This means a significant amount of solar radiation was blocked by the perovskite thermochromic window. The temperature inside the model house with the smart window was always lower than that of the model house with the normal window until 16:30 pm. For the second and third test results (14/06/2019, average relative humidity: 76%; 15/06/2019, average relative humidity: 74%), the temperature reduction was about 2.2 °C and 2.4 °C respectively in the morning. However, there was no

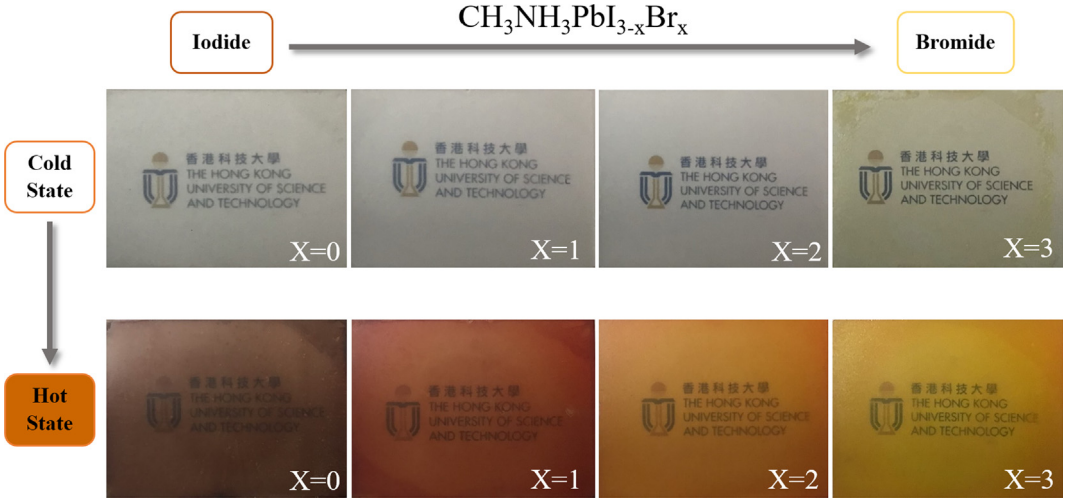

Fig. 11. The optical photographs of $CH_3NH_3PbI_{3-x}Br_x$ perovskite smart windows. The films were deposited on normal slide glass, demonstrating that the color of perovskite can be easily tuned by changing different halogen elements.

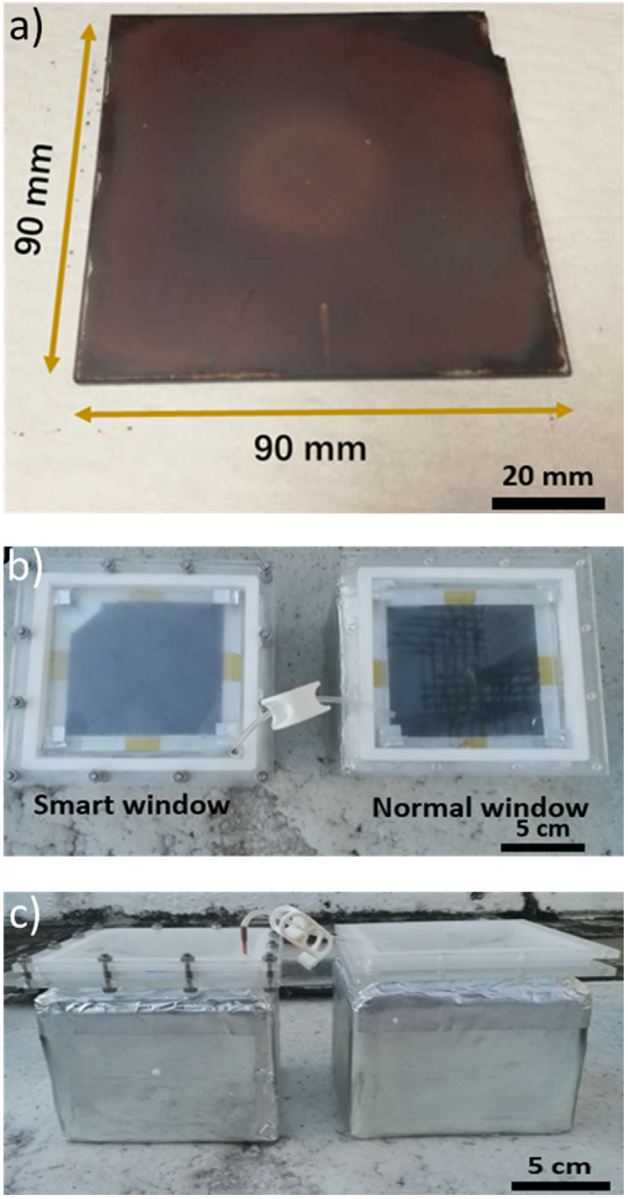

Fig. 12. (a) The prepared 90 × 90 mm perovskite smart window in hot state for the model house experiment; (b) top view: model house experimental setup; (c) front view.

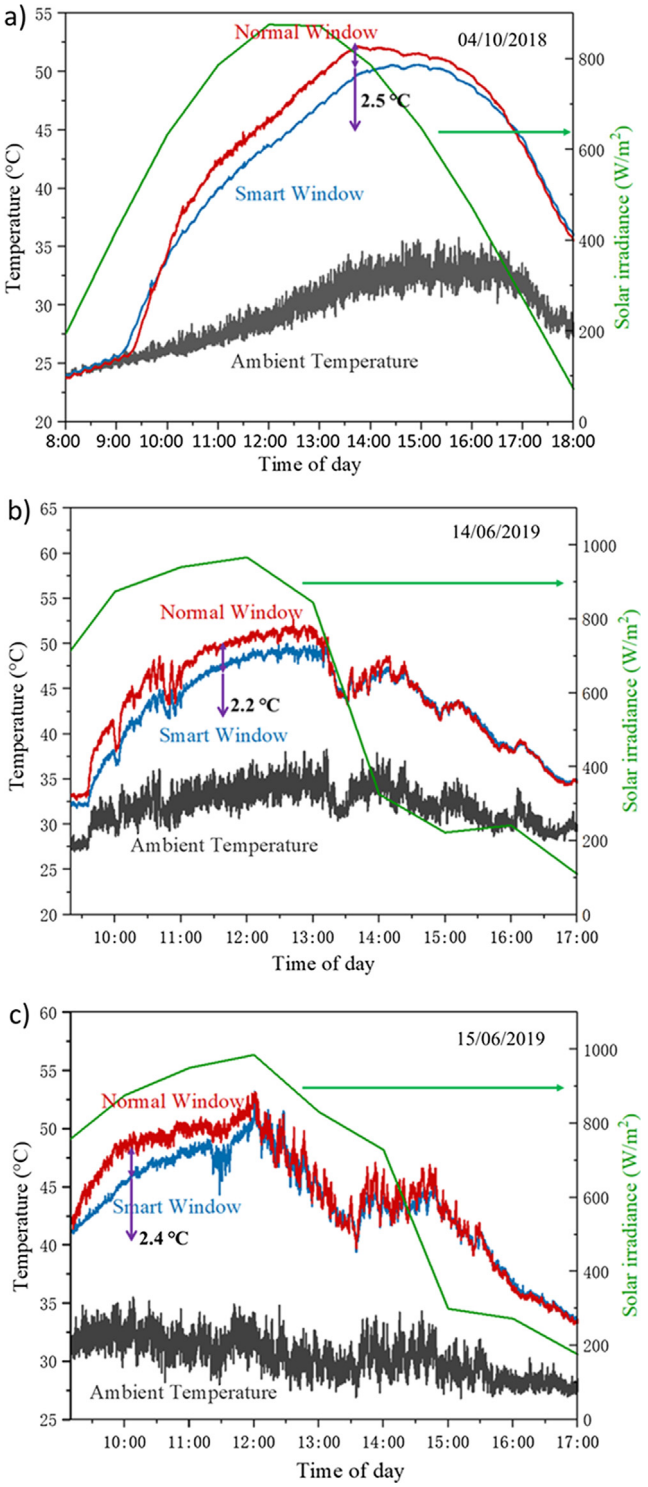

Fig. 13. Temperature as a function of irradiation time for perovskite smart windows and reference window with pure quartz. The solar irradiance data was also provided.

temperature difference for either the perovskite smart window or the normal window in the afternoon. This is because the weather became cloudy and the solar irradiance suddenly dropped from 13:00 on 14/06/2019 and 12:00 on 15/06/2019. It should be noted that thermochromic smart windows mitigate energy loss through modulating the short-wavelength solar radiation. When the solar irradiance is low, most of the energy is lost through windows was by other methods, such as conduction and convection. Therefore, at this condition, there is no difference between the thermochromic smart window and the normal window. All in all, based on the field test results obtained over the three different days, the designed perovskite thermochromic smart windows are effective to block the solar radiation showing considerable potential as energy-efficient solar modulating windows.

3.7. Comparison with other thermochromic smart window techniques

Fig. 14 displays the ΔT_{sol} and T_{lum} for different types of smart windows which have been reported. Much effort has been spent to lower the transition temperature and improve the optical performance. However, due to the characteristics of VO_2 (intrinsic yellowish color, thermochromism is only in the near infrared region), it is rather difficult to further improve the performance of VO_2 smart windows through different technologies, such as multi-layered structure, porous film, composite film and so on. The suitable lower critical solution temperature (LCST) and ΔT_{sol} makes hydrogel and ionogel promising candidates for energy-efficient smart windows. However, hydrogel and

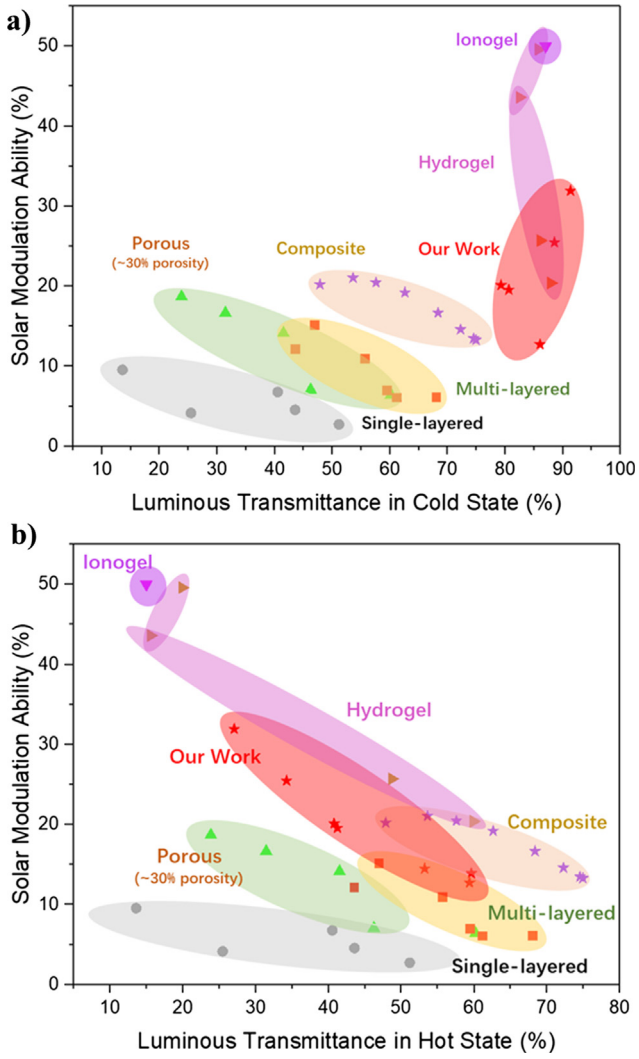

Fig. 14. (a) ΔT_{sol} against $T_{lum,cold}$ of different thermochromic smart windows; (b) ΔT_{sol} against $T_{lum,hot}$ of different thermochromic smart windows including single-layered VO_2 smart windows, multilayered VO_2 smart windows, porous VO_2 smart windows, composite VO_2 smart windows, hydrogel smart windows, ionogel smart windows and perovskite smart windows in this work.

ionogel are in liquid phase and require rigorous encapsulation, a problem that still needs to be resolved. However, the idea that they expand the thermochromism from the near infrared region to the visible region laid a good foundation for this work. Above all, the optical performance (i.e. $\Delta T_{sol} = 25.5\%$ at $T_{lum,hot} = 34.3\%$ & $\Delta T_{sol} = 12.7\%$ at $T_{lum,hot} = 59.4\%$ for different spin speeds and mixing ratios of PbI_2 and CH_3NH_3I) of the current perovskite smart windows is extremely competitive for thermochromic smart windows.

4. Conclusions

In this study, a perovskite thermochromic smart window is developed. The perovskite smart window is highly transparent at room temperature, with a record of luminous transmittance up to 91%. By changing the mixing ratio of PbI_2 and CH_3NH_3I, along with the spin speed, the results can vary between 34.3% and 59.6% for luminous transmittance in hot state and between 12.7% and 25.5% for solar modulation ability. The optimal mixing ratio of PbI_2 and CH_3NH_3I is chosen as 1:4 with a spin speed of 2000 rpm for the fabrication process. The transition temperature hysteresis of the perovskite smart window has been measured and results show that transition temperature depends on the relative humidity in the environment. When the relative humidity is less than 60%, the transition temperature can be reduced to less than 43 °C. Perovskite transition time of less than 5 min is also very satisfactory. In addition, the flexibility in the color for the proposed perovskite smart windows adds aesthetic value to the technology. According to the field test under direct sunlight in Hong Kong, the perovskite smart window can help reduce the indoor air temperature by as much as 2.5 °C compared to normal windows. The most typical alternative is the VO_2 thermochromic smart window. Compared to VO_2 smart windows, perovskite thermochromic smart windows shift the thermochromism from the NIR region to the mainly visible region, which leads to a larger solar modulation ability since half of the photons lie in this spectral region. Also, in the cold state, perovskite smart windows are almost transparent, making them suitable for winter applications by providing a sufficient visual portal for residents. However, the transition temperature of the perovskite is still too high to achieve the best energy saving performance. Although we found that decreasing the relative humidity decreases the transition temperature, the lower limit still needs to be further explored to achieve a better energy-saving performance. Overall, thanks to the high luminous transmittance, high solar modulation ability and solid phase of the smart windows, the proposed perovskite thermochromic smart windows have potential to meet the targets for real applications. Another point that needs further enhancement is the long-term stability. Future work is needed to study how to expand the thermochromism of the perovskite smart window to the near infrared wavelength to further increase the solar modulation ability and how to further decrease the transition temperature of the perovskite smart window such that a larger temperature reduction can be obtained. This high-performing thermochromic perovskite material opens a way to develop thermochromic smart windows.

Acknowledgements

The funding sources for this research are provided by the Hong Kong Research Grant Council via Collaborative Research Fund (CRF) account C6022-16G and General Research Fund (GRF) account 16200518.

References

[1] Grynning S, Time B, Uvsløkk SJPrtbpwtRCoZEB. An overview and some reflections on energy saving potentials by heat loss reduction through the building envelope. Project report to be published within the Research Centre on Zero Emission Buildings; 2011.
[2] Attia S, Favoino F, Loonen R, Petrovski A, Monge-Barrio AJABS. Adaptive façades system assessment: An initial review. Adv Build Skins 2015:1265–73.
[3] Somani PR, Radhakrishnan S. Electrochromic materials and devices: present and future. Mater Chem Phys 2003;77:117–33.
[4] Yao JN, Hashimoto K, Fujishima A. Photochromism induced in an electrolytically pretreated Mo03 thin film by visible light. Nature 1992;355:624–6.
[5] Ke Y, Zhou C, Zhou Y, Wang S, Chan SH, Long Y. Emerging thermal-responsive materials and integrated techniques targeting the energy-efficient smart window application. Adv Funct Mater 2018;1800113.
[6] Mlyuka NR, Niklasson GA, Granqvist CG. Thermochromic multilayer films of VO_2 and TiO_2 with enhanced transmittance. Sol Energy Mater Sol Cells 2009;93:1685–7.
[7] La T-G, Li X, Kumar A, Fu Y, Yang S, Chung H-J. Highly flexible, multipixelated thermosensitive smart windows made of tough hydrogels. ACS Appl Mater Interfaces 2017;9:33100–6.
[8] Zhou Y, Cai Y, Hu X, Long Y. Temperature-responsive hydrogel with ultra-large solar modulation and high luminous transmission for “smart window” applications. J Mater Chem A 2014;2:13550–5.
[9] Yang Y-S, Zhou Y, Chiang FBY, Long Y. Temperature-responsive hydroxypropylcellulose based thermochromic material and its smart window application. RSC Adv 2016;6:61449–53.
[10] Jain K, Vedarajan R, Watanabe M, Ishikiriyama M, Matsumi N. Tunable LCST behavior of poly (N-isopropylacrylamide/ionic liquid) copolymers. Polym Chem 2015;6:6819–25.
[11] Lee HY, Cai Y, Velioglu S, Mu C, Chang CJ, Chen YL, et al. Thermochromic ionogel: a new class of stimuli responsive materials with super cyclic stability for solar modulation. Chem Mater 2017;29:6947–55.
[12] Aries MBC, Veitch JA, Newsham GR. Windows, view, and office characteristics predict physical and psychological discomfort. J Environ Psychol 2010;30:533–41.
[13] Konstantzos I, Tzempelikos A, Chan Y-C. Experimental and simulation analysis of

daylight glare probability in offices with dynamic window shades. Build Environ 2015;87:244–54.
[14] Hopkinson RG. Glare from daylighting in buildings. Appl Ergon 1972;3:206–15.
[15] Taylor A, Parkin I, Noor N, Tummeltshammer C, Brown MS, Papakonstantinou I. A bioinspired solution for spectrally selective thermochromic VO_2 coated intelligent glazing. Opt Express 2013;21:A750–64.
[16] Ye H, Meng X, Xu B. Theoretical discussions of perfect window, ideal near infrared solar spectrum regulating window and current thermochromic window. Energy Build 2012;49:164–72.
[17] Halder A, Choudhury D, Ghosh S, Subbiah AS, Sarkar SK. Exploring thermochromic behavior of hydrated hybrid perovskites in solar cells. J Phys Chem Lett 2015;6:3180–4.
[18] Lin J, Lai M, Dou L, Kley CS, Chen H, Peng F, et al. Thermochromic halide perovskite solar cells. Nat Mater 2018;17:261–7.
[19] Dietrich MK, Kuhl F, Polity A, Klar PJ. Optimizing thermochromic VO2 by co-doping with W and Sr for smart window applications. Appl Phys Lett 2017;110:141907.
[20] Li S-Y, Niklasson GA, Granqvist CG. Thermochromic undoped and Mg-doped VO_2 thin films and nanoparticles: Optical properties and performance limits for energy efficient windows. J Appl Phys 2014;115:053513.
[21] Kang L, Gao Y, Luo H, Chen Z, Du J, Zhang Z. Nanoporous thermochromic VO_2 films with low optical constants, enhanced luminous transmittance and thermochromic properties. ACS Appl Mater Interfaces 2011;3:135–8.
[22] Xu G, Jin P, Tazawa M, Yoshimura K. Optimization of antireflection coating for VO_2-based energy efficient window. Sol Energy Mater Sol Cells 2004;83:29–37.
[23] Zhang Z, Gao Y, Luo H, Kang L, Chen Z, Du J, et al. Solution-based fabrication of vanadium dioxide on F: SnO_2 substrates with largely enhanced thermochromism and low-emissivity for energy-saving applications. Energy Environ Sci 2011;4:4290–7.
[24] Liu C, Wang S, Zhou Y, Yang H, Lu Q, Mandler D, et al. Index-tunable anti-reflection coatings: Maximizing solar modulation ability for vanadium dioxide-based smart thermochromic glazing. J Alloy Compd 2018;731:1197–207.
[25] Gao Y, Wang S, Kang L, Chen Z, Du J, Liu X, et al. VO_2–Sb:SnO_2 composite thermochromic smart glass foil. Energy Environ Sci 2012;5.
[26] Liu C, Balin I, Magdassi S, Abdulhalim I, Long Y. Vanadium dioxide nanogrid films for high transparency smart architectural window applications. Opt Express 2015;23:A124–32.
[27] Lu Q, Liu C, Wang N, Magdassi S, Mandler D, Long Y. Periodic micro-patterned VO_2 thermochromic films by mesh printing. J Mater Chem C 2016;4:8385–91.
[28] Qian X, Wang N, Li Y, Zhang J, Xu Z, Long Y. Bioinspired multifunctional vanadium dioxide: improved thermochromism and hydrophobicity. Langmuir 2014;30:10766–71.
[29] Zhou Y, Cai Y, Hu X, Long Y. VO_2/hydrogel hybrid nanothermochromic material with ultra-high solar modulation and luminous transmission. J Mater Chem A 2015;3:1121–6.
[30] Chen J, Xiong Y, Rong Y, Mei A, Sheng Y, Jiang P, et al. Solvent effect on the hole-conductor-free fully printable perovskite solar cells. Nano Energy 2016;27:130–7.
[31] Wang Y, Chen E, Lai H, Lu B, Hu Z, Qin X, et al. Enhanced light scattering and photovoltaic performance for dye-sensitized solar cells by embedding submicron SiO_2/TiO_2 core/shell particles in photoanode. Ceram Int 2013;39:5407–13.
[32] Stöber W, Fink A, Bohn E. Controlled growth of monodisperse silica spheres in the micron size range. J Colloid Interface Sci 1968;26:62–9.
[33] Gao Y, Wang S, Luo H, Dai L, Cao C, Liu Y, et al. Enhanced chemical stability of VO_2 nanoparticles by the formation of SiO_2/VO_2 core/shell structures and the application to transparent and flexible VO_2-based composite foils with excellent thermochromic properties for solar heat control. Energy Environ Sci 2012;5:6104–10.
[34] Leguy AMA, Hu Y, Campoy-Quiles M, Alonso MI, Weber OJ, Azarhoosh P, et al. Reversible hydration of $CH_3NH_3PbI_3$ in films, single crystals, and solar cells. Chem Mater 2015;27:3397–407.
[35] Yang J, Xu Z, Ye H, Xu X, Wu X, Wang J. Performance analyses of building energy on phase transition processes of VO_2 windows with an improved model. Appl Energy 2015;159:502–8.
[36] Huang A, Zhou Y, Li Y, Ji S, Luo H, Jin P. Preparation of $V_xW_{1-x}O_2$(M)@ SiO_2 ultrathin nanostructures with high optical performance and optimization for smart windows by etching. J Mater Chem A 2013;1:12545–52.
[37] Ke Y, Balin I, Wang N, Lu Q, Tok AIY, White TJ, et al. Two-dimensional SiO_2/VO_2 photonic crystals with statically visible and dynamically infrared modulated for smart window deployment. ACS Appl Mater Interfaces 2016;8:33112–20.
[38] Saeli M, Piccirillo C, Parkin IP, Ridley I, Binions R. Nano-composite thermochromic thin films and their application in energy-efficient glazing. Sol Energy Mater Sol Cells 2010;94:141–51.
[39] Hwang K, Jung YS, Heo YJ, Scholes FH, Watkins SE, Subbiah J, et al. Toward large scale roll-to-roll production of fully printed perovskite solar cells. Adv Mater 2015;27:1241–7.
[40] Meroni SMP, Mouhamad Y, De Rossi F, Pockett A, Baker J, Escalante R, et al. Homogeneous and highly controlled deposition of low viscosity inks and application on fully printable perovskite solar cells. Sci Technol Adv Mater 2017;19:1–9.
[41] Yang Z, Chueh C-C, Zuo F, Kim JH, Liang P-W, Jen AKY. High-performance fully printable perovskite solar cells via blade-coating technique under the ambient condition. Adv Energy Mater 2015;5.
[42] Goia F. Search for the optimal window-to-wall ratio in office buildings in different European climates and the implications on total energy saving potential. Sol Energy 2016;132:467–92.
[43] Wang M, Gao Y, Cao C, Chen K, Wen Y, Fang D, et al. Binary solvent colloids of thermosensitive poly(N-isopropylacrylamide) microgel for smart windows. Ind Eng Chem Res 2014;53:18462–72.
[44] Ji H, Liu D, Cheng H, Zhang C. Inkjet printing of vanadium dioxide nanoparticles for smart windows. J Mater Chem C 2018;6:2424–9.
[45] Ye H, Long L, Zhang H, Xu B, Gao Y, Kang L, et al. The demonstration and simulation of the application performance of the vanadium dioxide single glazing. Sol Energy Mater Sol Cells 2013;117:168–73.